

Transfer Learning for Lung Nodules Classification with CNN and Random Forest

Abdulrazak Yahya Saleh^{1*}, Chee Ka Chin² and Ros Ameera Rosdi¹

¹Faculty of Cognitive Sciences and Human Development, Universiti Malaysia Sarawak (UNIMAS), 94300 Kota Samarahan, Sarawak, Malaysia

²Department of Electrical and Electronic, Faculty of Engineering, Universiti Malaysia Sarawak (UNIMAS), 94300 Kota Samarahan, Sarawak, Malaysia

ABSTRACT

Machine learning and deep neural networks are improving various industries, including healthcare, which improves daily life. Deep neural networks, including Convolutional Neural Networks (CNNs), provide valuable insights and support in improving daily activities. In particular, CNNs enable the recognition and classification of images from CT and MRI scans and other tasks. However, training a CNN requires many datasets to attain optimal accuracy and performance, which is challenging in the medical field due to ethical worries, the lack of descriptive notes from experts and labeled data, and the overall scarcity of disease images. To overcome these challenges, this work proposes a hybrid CNN with transfer learning and a random forest algorithm for classifying lung cancer and non-cancer from CT scan images. This research aims include preprocessing lung nodular data, developing the proposed algorithm, and comparing its effectiveness with other methods. The findings indicate that the proposed hybrid CNN with transfer learning and random forest performs better than standard CNNs without transfer learning. This research demonstrates the potential of using machine learning algorithms in the healthcare industry, especially in disease detection and classification.

Keywords: Convolutional Neural Network, CT scan, lung nodules, random forest, transfer learning

ARTICLE INFO

Article history:

Received: 17 May 2023

Accepted: 15 August 2023

Published: 03 November 2023

DOI: <https://doi.org/10.47836/pjst.32.1.25>

E-mail addresses:

ysahabdulrazak@unimas.my (Abdulrazak Yahya Saleh)

cheekachin@yahoo.com.my (Chee Ka Chin)

rosameerar@gmail.com (Ros Ameera Rosdi)

*Corresponding author

INTRODUCTION

Lung cancer is a common and deadly disease in modern times. Cancer cells initially develop in the lungs but can spread to other organs, including lymph nodes and the brain (Rajadurai et al., 2020). Lung cancer was the most common and deadly cancer worldwide in 2018, making up 11.6% of all cancer cases and deaths (Bray

et al., 2018). It was also Malaysia's second leading cause of death from cancer that year, after breast cancer (Bray et al., 2018), according to the World Health Organization. Men comprise approximately 16.6% of the patients, while women comprise 5.4%. In Malaysia, lung cancer is the third most prevalent type of cancer, affecting men more than women, according to the Malaysia National Cancer Registry Report 2012-2016 (Azizah et al., 2019). Today, Deep Learning is often used in medical image analysis (Alom et al., 2019; Arabahmadi et al., 2022; Salahuddin et al., 2022; Zakaria et al., 2022). Deep Learning is becoming increasingly popular and necessary for reliable and accurate results (Anderson et al., 2018). Deep learning simulates how the human brain processes data and recognizes patterns to make decisions. As technology and algorithms improve, machines can offer more accurate and reliable medical analysis. Identifying cells that are cancerous or malignant is essential for lung cancer therapy.

Literature Review

Deep learning techniques can analyze CT scan images and identify cancer cells at an early stage to prevent them from becoming fatal (Primakov et al., 2022; Thai et al., 2021). Deep learning image analysis applications on Computed Tomography (CT) scan images to aid in the detection of malignant cells prior to their development and lethality (Primakov et al., 2022; Thai et al., 2021). Deep Learning is ideally suited for image processing tasks, especially object detection and localization (Singh & Gupta, 2019). Deep learning, especially CNN, can achieve high accuracy with abundant data (Zhao et al., 2018). Convolutional Neural Networks (CNNs) need large and precise labeled training data, such as ImageNet, to operate effectively. Unfortunately, large datasets are often unavailable for medical images because of the high cost of expert explanations, ethical concerns, and the lack of images of diseases (Zhao et al., 2018). In addition, models with a high parameter count tend to overfit and cannot learn patterns when working with lesser datasets (Li et al., 2020). Most traditional CNN architectures begin with a high parameter count, making their performance highly dependent on the data size. Therefore, datasets that consist of only hundreds or thousands of instances are incompatible with standard CNN models trained on large-scale datasets like ImageNet (Keshari et al., 2018). It is an issue that researchers need to address if they want to improve the performance of the model when handling a huge volume of annotated data. A standard CNN may prove insufficient in medical imaging with small datasets, where datasets usually comprise a few hundred to thousands of data. Numerous studies have investigated various types of CNN for lung nodule detection, false positive reduction, and classification to address this issue (Halder et al., 2020; Forte et al., 2022; Nakrani et al., 2021; Sharif et al., 2020). However, Table 1 in this document focuses specifically on CNNs employing innovative strategies instead of conventional techniques or conventional CNNs.

Table 1

A comprehensive review of various types of CNN for pulmonary nodule detection

	Ref.	Model	Data sets	Key Points
Hybrid CNN	Zhao et al. (2018)	2D LeNet + 2D AlexNet	LIDC/IDRI	A malignancy prediction model was created by combining the settings of the LeNet layers with the parameter settings of AlexNet.
Transfer Learning Based System	Da Nóbrega et al. (2018)	2D CNN, SVM, MLP, KNN, RF, Naïve Bayes	LIDC/IDRI	Eleven 2D CNN models are utilized for feature extraction. Models are ResNet50, DenseNet169, VGG16, Xception, VGG19, Inception-ResNet-V2, DenseNet201, MobileNet, InceptionV3, NASNetMobile and NASNetLarge .SVM, MLP, KNN, RF, and Naïve Bayes are trained separately with collected features.
	Yamashita et al. (2018)	VGG16	LIDC/IDRI Private Data set	Comparison of CNN models for feature extraction, models based on feature engineering, and models based on transfer learning
Multiscale Feature with Transfer Learning	Tang et al. (2020)	3D U-Net CNN, Transfer learning	TIANCHI17 and LUNA16	In the study, 3D U-Net architecture was used to extract features from input images. Transfer learning was also utilized, and fine-tuning the model helped feature extraction. The experiment showed that layer-wise transfer training improved image recognition accuracy in situations with a limited sample size.
Advanced Off-The-Shelf CNNs	Ali et al. (2018)	3D CNN	LUNA16	Reinforcement learning for medical image analysis and lung nodule detection in CT scan images is a groundbreaking advance.
	Qin et al. (2018)	3D U-Net and 3D DenseNet	LUNA 16	Automatic lung nodule detection combines multitasking residual learning and online mining techniques for hard negative examples, including a 2D U-Net, a 3D DenseNet, and a Region Proposal Network (RPN). The 3D U-Net generates candidate nodes, while the 3D DenseNet is mainly used to reduce false positives.
	Tang et al. (2018)	3D Faster R-CNN and 3D DCNN	Tianchi AI competition	A two-phased framework is used to identify nodules and reduce false positives. The framework utilizes a 3D Faster RCNN to generate nodule samples and a 3D DCNN model to recognize nodule candidates.

Numerous studies have aimed to enhance the precision of early lung cancer detection through Deep Learning. However, there is still a discrepancy between identifying these algorithms and their integration into real medical applications. A hybrid deep learning model has been developed based on Convolutional Neural Networks (CNNs) and Random Forest (RF) for malicious node classification. The reason for using this hybrid approach is that transfer learning is advantageous when dealing with limited data and can leverage knowledge from pre-trained models, while RF offers robustness, feature importance analysis, versatility, and competitive performance across different types of tasks. Our model uses transfer learning from pre-trained CNN models to extract features from node images. The model's performance was evaluated compared to a baseline CNN model without transfer learning.

MATERIALS AND METHODS

The study is divided into four phases: Dataset Preparation, Research Design, Application and Implementation, and Performance Analysis. The research methodology is presented in Figure 1, while Figure 2 shows the overall framework for the suggested model.

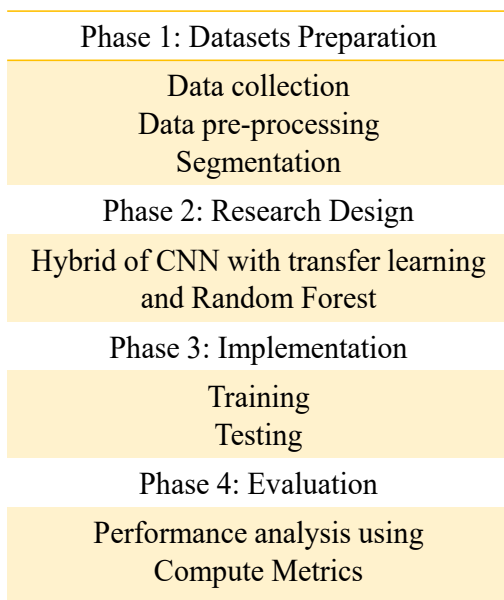


Figure 1. The research methodology employed in the study's workflow

LIDC-IDRI dataset, with different factors used to filter the heterogeneous scans. Due to the minuscule size of pulmonary nodules, only a 2.5 mm slice thickness CT scan or less was considered. CT scans that demonstrated non-uniform slice spacing or missing slices

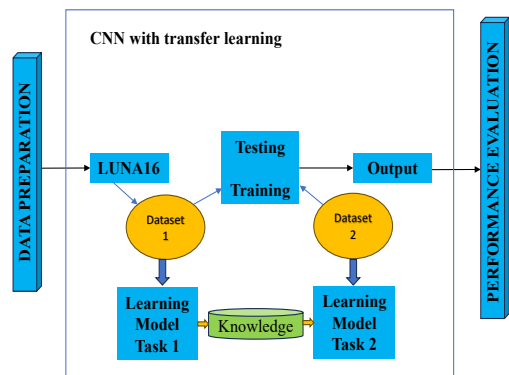


Figure 2. The overarching structure for the proposed methods

This research uses a subset of the LIDC-IDRI dataset known as LUNA16 (Camp, 2022). We use the LUNA16 dataset, a widely used lung cancer CT image dataset, and a subset of the LIDC-IDRI dataset.

The LUNA16 dataset is a subset of the LIDC-IDRI dataset, with different factors used to filter the heterogeneous scans. Due to the minuscule size of pulmonary nodules, only a 2.5 mm slice thickness CT scan or less was considered. CT scans that demonstrated non-uniform slice spacing or missing slices

were excluded from the analysis. As a result, the dataset was reduced to 888 CT scans annotated by radiologists, resulting in 36,378 annotations. Only annotations classified as nodules 3 mm were deemed relevant in lung cancer screening protocols. When multiple readers discovered nodules that were close together, their radii were combined, and their positions and diameters averaged.

Lung segmentation data are also provided, consisting of lung segmentation images calculated with automatic algorithms (Peirelinck et al., 2022). However, these segmentation images should not be utilized as the gold standard for any segmentation study. It is worth noting that the primary dataset via LIDC-IDRI was saved in DICOM (.dcm) format, an alternative format for CT scan data. The model was trained with 1528 training datasets, while the remaining CT scans of patients were used for testing and validation. In total, there were 478 test datasets and 382 validation datasets. Figure 3 shows disparate sections from a LUNA16 CT scan.

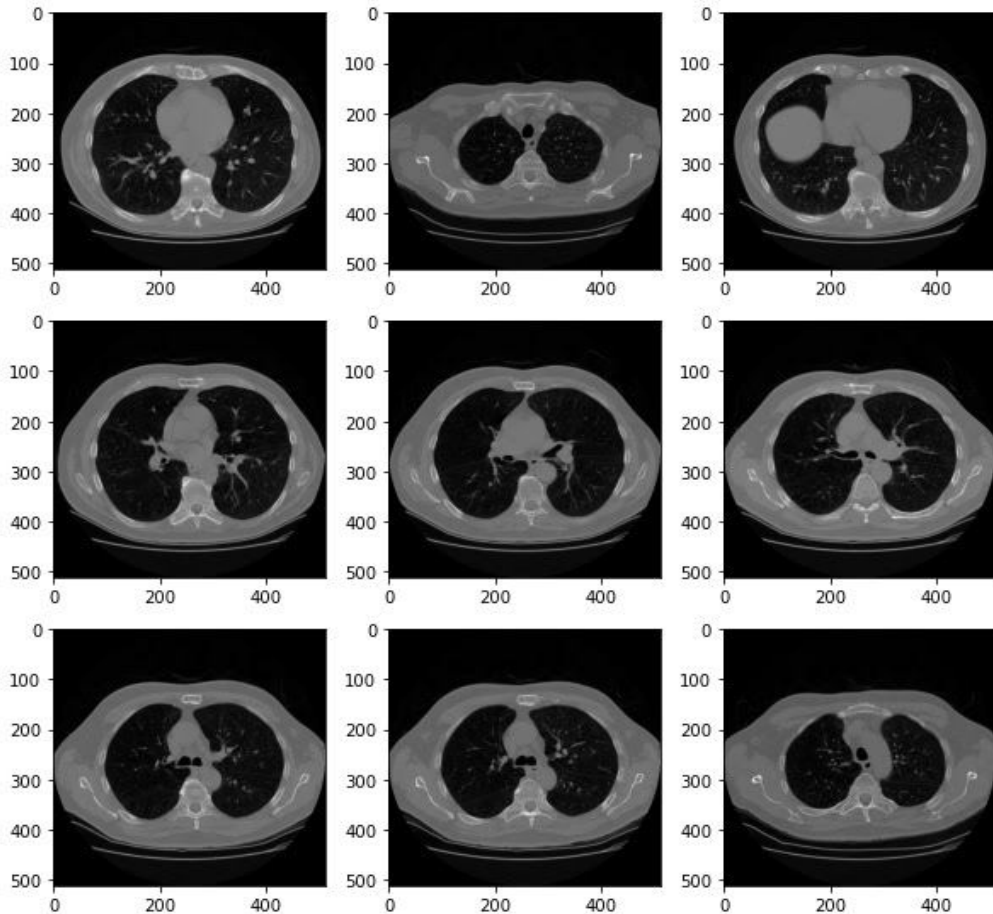


Figure 3. Primary CT scan DICOM slices extraction from LUNA16 dataset

This research employed a pre-trained VGG16 model, trained on 1.2 million natural images from the ImageNet dataset. VGG16 is initially pretrained on the large-scale ImageNet dataset, which contains millions of labeled images from various categories. During pretraining, the model learns to extract useful features from the images and classify them into one of the ImageNet classes. This pretraining step helps VGG16 learn general visual representations that can be applied to various tasks. The overall prediction of VGG16, $VGG16(x)$, can be represented as:

$$VGG16(x) = FC(h\{M - 1\}) \quad (1)$$

Where FC represents the last fully connected layer, x is the input image, M is the total number of fully connected layers, and $h\{M - 1\}$ is the input to the last fully connected layer. A comprehensive framework was developed for the proposed methods in this study, with a CNN algorithm utilized to leverage the LUNA16 dataset for lung nodule classification.

The proposed algorithm utilizes Convolutional Neural Networks (CNN) with transfer learning and is fed the LUNA16 dataset as input. The proposed algorithm used transfer learning, a popular method in which pre-trained models established for one task are used as the basis for another model for a different task (Goodfellow et al., 2016). In addition, transfer learning is also a machine learning technique that involves leveraging knowledge gained from one task or domain and applying it to a different but related task or domain. It enables the reuse of pre-trained models and learned representations, which can significantly benefit new tasks, especially when the new task has limited training data. The underlying idea of transfer learning is that knowledge gained from solving one task can be transferred and utilized to improve the learning or performance of another related task. Instead of starting the learning process from scratch, transfer learning allows models to initialize with already learned features or parameters, speeding up convergence and improving generalization. Transfer learning θ_t typically involves fine-tuning the pre-trained model on the target task. It can be represented as:

$$\theta_t = \operatorname{argmin}(\theta_t)L(\theta_t, D) + \alpha L(\theta_p + D_p) \quad (2)$$

Where D is the target task training set, $L(\theta_t, D)$ is the loss function for the target task, α is a trade-off parameter, θ_p is the weights and biases of the pre-trained model, D_p is a separate pretraining dataset (or a subset of the target task data), and $L(\theta_p + D_p)$ represents the loss function for pretraining.

Two prevalent transfer learning techniques exist the developed model approach and the pre-trained model approach (Peirelinck et al., 2022; Zhuang et al., 2020). Previous research has demonstrated that transfer learning can enhance the discriminative capabilities of a generic dataset and improve the model's ability to generalize to other tasks (Da Nóbrega et al., 2018).

Various scholars have also shown interest in hybridization techniques due to their recent outstanding performance in addressing cancer detection problems by enhancing algorithm performance (Chin et al., 2021a, 2021b; Saleh et al., 2021). Therefore, the proposed approach for classifying lung nodules involves utilizing a hybrid CNN with transfer learning and Random Forest (RF). Random Forest (RF) is a popular machine-learning algorithm for classification and regression tasks. An ensemble learning method combines multiple decision trees to make predictions. The prediction of the random forest $RF(x)$ can be represented as:

$$RF(x) = \operatorname{argmax}(c) \sum t(x) R \quad (3)$$

Where $t(x)$ is the prediction of the t -th decision tree for input x , and c represents the possible classes or outputs.

The Python programming language was used to train and test the algorithm, followed by a comprehensive performance metrics evaluation. After dataset preparation and research design, the proposed algorithm underwent training and testing, and the resulting models were evaluated based on performance. The hybrid method is implemented using Python programming on a computer system with an Intel Core i5 10th Gen processor, 16 GB RAM, and NVIDIA GeForce RTX 2060 GPU support with 6 GB RAM. The optimal hyperparameters that need to be set for this research include the number of trees, which is set to three, and the random state, which is set to 42, in the function of the random forest. The dataset is divided into two groups, namely the Train set and Test set, with most of the dataset allocated to training and the remaining portion reserved for model testing. The performance measure metrics are also analyzed based on testing accuracy, sensitivity, specificity, and F1-score, which can be represented as:

$$\text{Testing Accuracy} = \frac{TP + TN}{TP + TN + FP + FN} \quad (4)$$

$$\text{Sensitivity} = \frac{TP}{TP + FN} \quad (5)$$

$$\text{Specificity} = \frac{TN}{TN + FP} \quad (6)$$

Where TP , TN , FP , and FN are True Positive, True Negative, False Positive, and False Negative, respectively.

RESULTS AND DISCUSSION

The library pydicom is used to demonstrate the image field and the metadata information in the CT scan images to visualize the dataset. As the images have been deposited in

DICOM format, a standard browser cannot be used to access them. An example of the metadata stored in the file is shown in Figure 4. The watershed algorithm has been utilized to segment the dataset. The watershed algorithm has been considered a traditional image segmentation and separation algorithm. In image processing, the grayscale image can be subjected to a procedure similar to a geological watershed or drainage split, which divides adjacent drainage basins. This procedure, aptly named "watershed," employs the image as though it had been a topographic map, with each point's brightness denoting its height. As a result, it becomes possible to identify lines that follow the crests of ridges. In 1997, M. Couprie and G. Bertrand coined the term "topological watershed." The watershed algorithm begins with user-defined markers and treats pixel values as a local topography (elevation) (Bertrand, 2005).

```

-----
(0008, 0005) Specific Character Set          CS: 'ISO_IR 100'
(0008, 0016) SOP Class UID                  UI: CT Image Storage
(0008, 0018) SOP Instance UID               UI: 1.2.840.113654.2.55.247817952625791837963403492891187883824
(0008, 0060) Modality                       CS: 'CT'
(0008, 103e) Series Description              LO: 'Axial'
(0010, 0010) Patient's Name                 PN: '00cba091fa4ad62cc3200a657aeb957e'
(0010, 0020) Patient ID                     LO: '00cba091fa4ad62cc3200a657aeb957e'
(0010, 0030) Patient's Birth Date           DA: '19000101'
(0018, 0060) KVP                             DS: None
(0020, 000d) Study Instance UID              UI: 2.25.86208730140539712382771890501772734277950692397709007305473
(0020, 000e) Series Instance UID            UI: 2.25.11575877329635228925808596800269974740893519451784626046614
(0020, 0011) Series Number                   IS: "3"
(0020, 0012) Acquisition Number              IS: "1"
(0020, 0013) Instance Number                 IS: "134"
(0020, 0020) Patient Orientation             CS: ''
(0020, 0032) Image Position (Patient)        DS: [-145.500000, -158.199997, -356.200012]
(0020, 0037) Image Orientation (Patient)     DS: [1.000000, 0.000000, 0.000000, 0.000000, 1.000000, 0.000000]
(0020, 0052) Frame of Reference UID          UI: 2.25.83033509634441686385652073462983801840121916678417719669650
(0020, 1040) Position Reference Indicator    LO: 'SN'
(0020, 1041) Slice Location                  DS: "-356.200012"
(0028, 0002) Samples per Pixel               US: 1
(0028, 0004) Photometric Interpretation      CS: 'MONOCHROME2'
(0028, 0010) Rows                            US: 512
(0028, 0011) Columns                          US: 512
(0028, 0030) Pixel Spacing                    DS: [0.597656, 0.597656]
(0028, 0100) Bits Allocated                   US: 16
(0028, 0101) Bits Stored                      US: 16
(0028, 0102) High Bit                         US: 15
(0028, 0103) Pixel Representation             US: 1
(0028, 0120) Pixel Padding Value              US: 63536
(0028, 1050) Window Center                    DS: "40.0"
(0028, 1051) Window Width                     DS: "400.0"
(0028, 1052) Rescale Intercept                DS: "-1024.0"
(0028, 1053) Rescale Slope                   DS: "1.0"
(7fe0, 0010) Pixel Data                       OW: Array of 524288 elements
-----

```

Figure 4. The metadata is stored within a solitary DICOM file

The Watershed algorithm floods the basins of various markers until they intersect on watershed lines. Often, these markers have been selected as local minima in an image, and the basins are filled accordingly. This semantic segmentation approach helps emphasize the lung area and generate binary masks. To begin, external and internal markers from the images of CT scans were obtained using binary dilations and then added to a full dark image using watershed methods. The watershed marker eliminates image noise and detects cancerous cells in the lungs. The removal of external noise from the images is illustrated

in Figure 5, where a binary mask is applied to the image, with black pixels indicating cancer cells. An integrated Sobel filter and watershed algorithm were used to improve segmentation to remove the outer lung layers. An internal marker is then used to create a lung filter using Numpy's bitwise operations, which extracts the heart from the CT scan images. To ensure more accurate segmentation than previous methods, morphological operations, and gradients are used to complete the lung filter. Figure 6 displays the segmented lung after applying the Sobel filter application. The process created 2388 labeled images comprising almost 12 patients with CT scan data, with a comparable number of cancerous and non-cancerous patients.

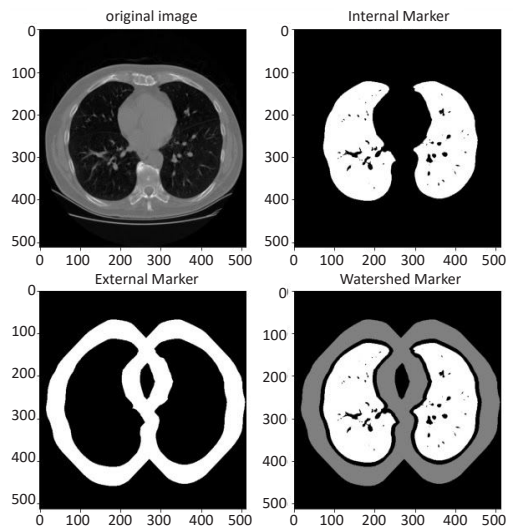


Figure 5. Distinct markers are derived from the watershed algorithm applied to the CT scan

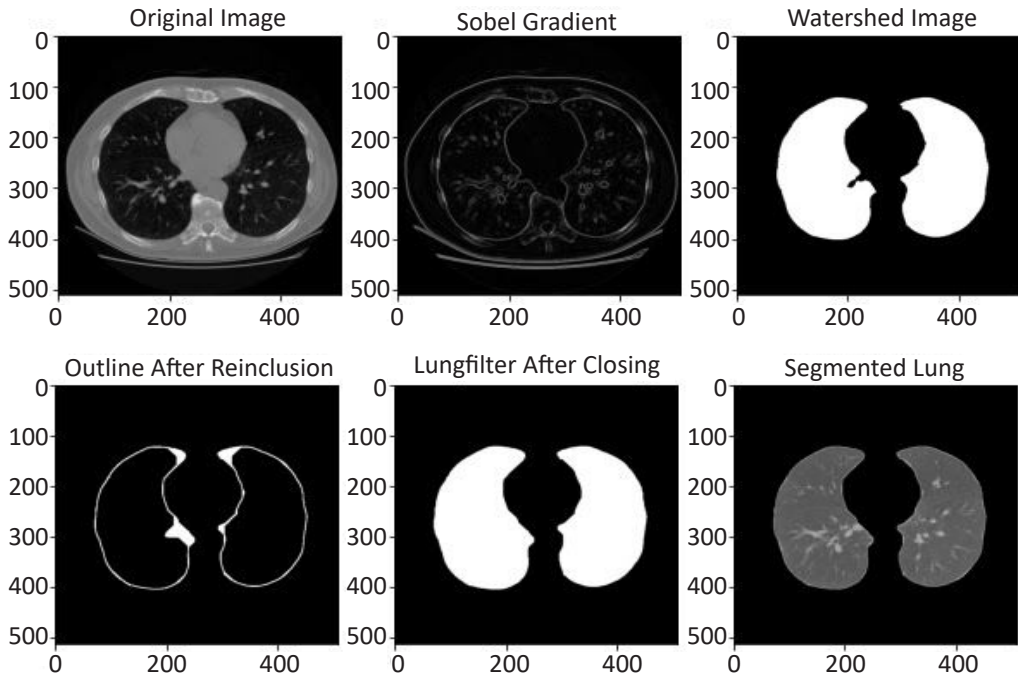


Figure 6. Visualization of lung segmentation

The model that was suggested is a combination of two powerful techniques: CNN with transfer learning and Random Forest. In order to contrast the performance of both models, a standard CNN was built as the first model, which uses convolution layers, flattened fully connected layers, max pooling, and dropout in the middle layers. Figure 7 illustrates this basic approach without the advantage of transfer learning. The second hybrid model applies transfer learning on a pre-trained VGG-16 model and Random Forest as a classifier. The last three layers were modified to incorporate the Random Forest classifier. The base estimator used in this hybrid model is 3, with a random state 42. Figure 8 displays the illustration of the suggested model. Subsequently, the dual models, one with Transfer Learning and the other with Random Forest, were implemented and trained on segmented lungs. A batch size of 64 was used for the image data generator, and 20 images were used in each epoch for 30 epochs, except for the first model, which had 20 images in each epoch. The shape of the training images for the first model was (32,32,3) while the proposed model had a shape of (128,128,3). The application of augmentation techniques facilitated the training of models on various augmentations, including shear range, zoom range, horizontal flip, rotation range, and center shift, thereby achieving superior outcomes. In the final layer, a solitary binary classification node distinguishes between cancerous and non-cancerous lungs. Additionally, TensorFlow Keras callbacks were utilized to preserve the most accurate model and execute a comprehensive 30-epoch training session to chart the comparative graphs.

Table 2 compares the proposed hybrid model's testing accuracy and Area Under the Curve (AUC) and the standard CNN without transfer learning. The findings display that the proposed hybrid model beats the standard model and achieves better test accuracy and AUC. The proposed model is considered preferable over the standard model despite the fact

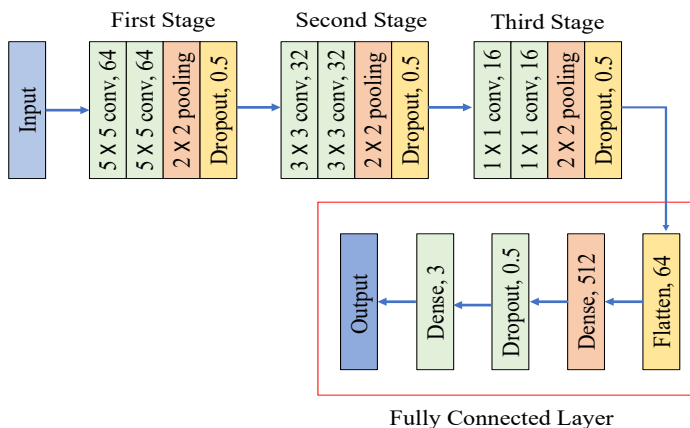


Figure 7. Standard CNN without transfer learning

that the standard model may still be suitable for solving classification tasks. Furthermore, Figure 9(a) shows that the proposed model attained an AUC of 0.985, better than the original model's AUC of 0.983, as shown in Figure 9(b).

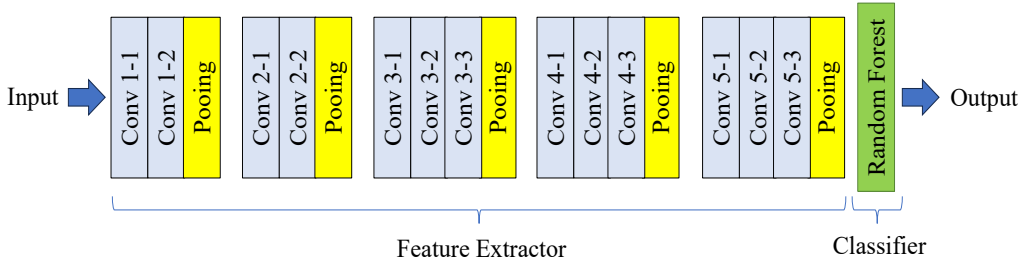


Figure 8. Hybrid CNN with transfer learning and Random Forest

Table 2
Overview of the accuracy performance of both models

Models	Testing Accuracy	Area Under the Curve (AUC)
Standard Model	93.72%	0.983
Proposed Model (Hybrid CNN with Transfer Learning and Random Forest)	98.53%	0.985

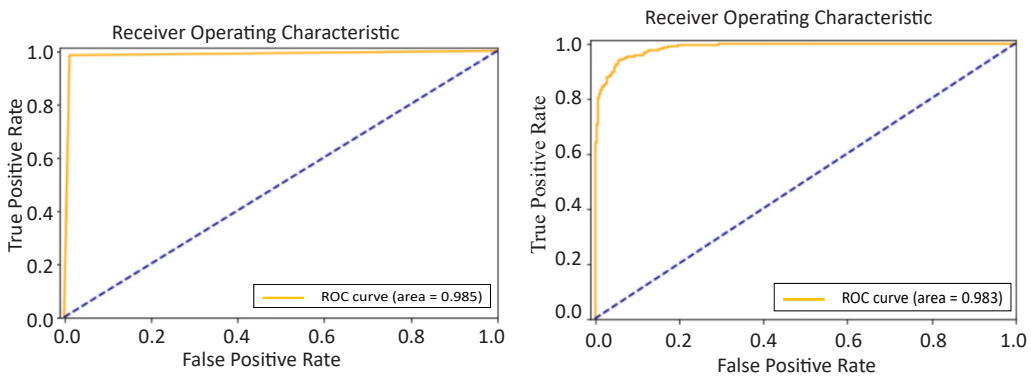


Figure 9. Receiver Operating Characteristic (ROC) Curve Performance (a) Proposed Hybrid Model (b) Standard Model

In terms of the confusion matrix, the hybrid model proposed in this study outperformed the typical CNN model without transfer learning in terms of accuracy. All of the CT scan images are classified correctly for the proposed hybrid model, as shown in Figure 10(a), while some of the CT scan images are still classified incorrectly for the standard CNN model, as shown in Figure 10(b). Based on Table 3, the performance metrics of CT image classification through the confusion matrix, as presented in Figure 10, proved that

the proposed hybrid model is better than the standard model. This confusion matrix and performance measures show that both models can classify most CT scan images. It can be proven in Figures 11(a) and 11(b), which are some CT scan images predicted correctly based on the standard and suggested models.

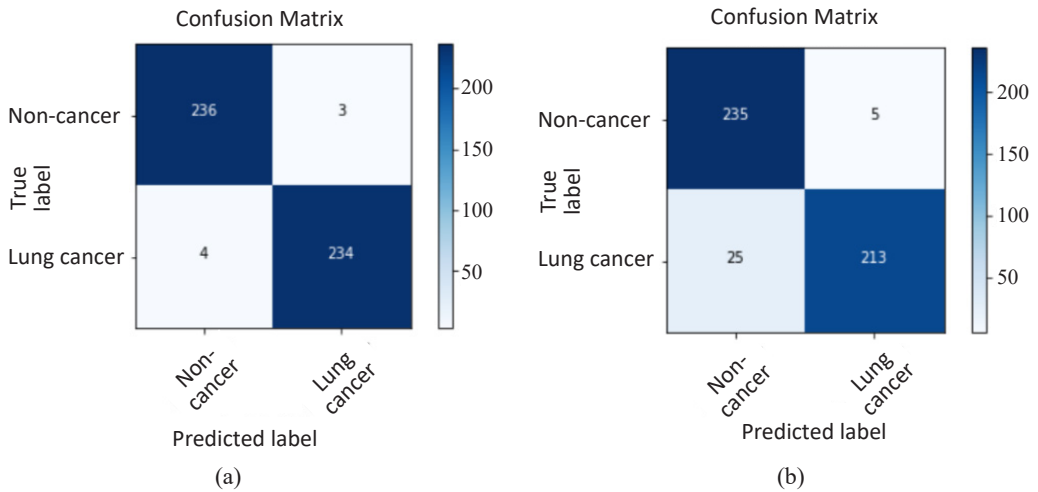


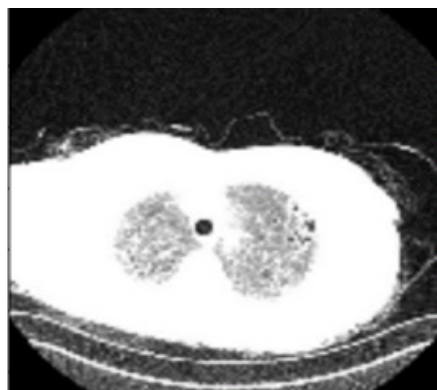
Figure 10. Confusion Matrix Performance (a) Proposed Hybrid Model (b) Standard Model

Table 3
Performance measure

Models	Sensitivity	Specificity	F1-Score
Standard Model	97.92%	89.54%	94.00%
Proposed Model (Hybrid CNN with Transfer Learning and Random Forest)	98.74%	98.32%	98.54%



(a)



(b)

Figure 11. Prediction and actual label are (a) non-cancer, (b) lung cancer

A comparative study in Table 4 shows that the proposed CNN with transfer learning and Random Forest model performs better than the existing techniques. Only work from (Saleh et al., 2021) performed better than the proposed hybrid work in specificity and AUC. During study development, several challenges arose that significantly impacted the results and outcomes. One of the biggest challenges was the dataset format used, which was in dmc format as opposed to ordinary formats of image processing such as jpg. The DMC format saves information about patients and a 3D CT scan image, so it was necessary to convert the images to jpg format before feeding them into the models for training and testing. It made the research more labor-intensive and time-consuming.

Table 4
Comparative study

Models	Testing Accuracy	Sensitivity	Specificity	F1-Score	AUC
3D U-Net CNN (Tang et al., 2020)	96.80%	92.40%	94.60%	-	0.941
3D CNN (Ali et al., 2018)	64.40%	58.90%	55.30%	-	-
3D U-Net and 3D DenseNet (Qin et al., 2018)	-	96.70%	-	-	-
Deformable CNN (Haiying et al., 2021)	-	95.80%	-	-	-
CNN (Sheng et al., 2021)	90.00%	-	-	-	-
AlexNet CNN (Agarwal et al., 2021)	96.00%	-	-	-	-
Deep Neural Networks Ensemble (Ardimento et al., 2021)	96.49%	98.73%	-	-	-
CNN-SVM (Saleh et al., 2021)	97.91%	97.90%	99.32%	-	1.000
Proposed Hybrid Model	98.53%	98.74%	98.32%	98.54%	0.985

CONCLUSION

Deep learning is crucial in acquiring profound knowledge and aiding medical professionals in comprehending a patient's condition, significantly enhancing their quality of life. The medical field has seen an increasing adoption of machine learning and deep neural networks due to their ability to improve detection and classification, ultimately benefiting patients. Convolutional Neural Networks (CNNs) have gained widespread popularity

in medical imaging applications, especially for CT and MRI scan analysis, recognition, and classification tasks. However, achieving high accuracy and performance with CNN algorithms requires extensive training using large datasets.

A hybrid CNN employing transfer learning and random forest techniques has been developed to improve lung nodule classification. This hybridization has shown promise in enhancing image classification. In the future, the hybrid algorithm will be applied to various medical imaging fields. This technique can benefit from a wide range of imaging modalities for improving image classification, detection, and segmentation.

ACKNOWLEDGEMENTS

The authors acknowledged the financial support from the Ministry of Higher Education Malaysia through the Fundamental Research Grant Scheme (FRGS) FRGS/1/2021/SS0/UNIMAS/02/4. Moreover, we thank the Faculty of Cognitive Sciences and Human Development, Universiti Malaysia Sarawak (UNIMAS), for their support and funding of the publication.

REFERENCES

- Agarwal, A., Patni, K., & Rajeswari, D. (2021, July 8-10). *Lung cancer detection and classification based on Alexnet CNN*. [Paper presentation]. International Conference on Communication and Electronics System (ICCES 2021), Coimbatre, India. <https://doi.org/10.1109/ICCES51350.2021.9489033>
- Ali, I., Hart, G. R., Gunabushanam, G., Liang, Y., Muhammad, W., Nartowt, B., Kane, M., Ma, X., & Deng, J. (2018). Lung nodule detection via deep reinforcement learning. *Frontiers in Oncology*, 8, 108. <https://doi.org/10.3389/fonc.2018.00108>
- Alom, M. Z., Taha, T. M., Yakopcic, C., Westberg, S., Sidike, P., Nasrin, M. S., Hasan, M., Essen, B. C. V., Awwal, A. A. S., & Asari, V. K. (2019). A state-of-the-art survey on deep learning theory and architectures. *Electronics*, 8(3), 292. <https://doi.org/10.3390/electronics8030292>
- Anderson, J., Rainie, L., & Luchsinger, A. (2018, December 10). *Artificial intelligence and the future of humans*. Pew Research Center. <chrome-extension://efaidnbmnnnibpajpglefindmkaj/http://tony-silva.com/eslefl/miscstudent/downloadpagearticles/AIhumanfuture-pew.pdf>
- Arabahmadi, M., Farahbakhsh, R., & Rezazadeh, J. (2022). Deep learning for smart healthcare—A survey on brain tumor detection from medical imaging. *Sensors*, 22(5), 1960. <https://doi.org/10.3390/s22051960>
- Ardimento, P., Aversano, L., Bernardi, M. L., & Cimitile, M. (2021, July 18-22). *Deep neural networks ensemble for lung nodule detection on chest CT scans*. [Paper presentation]. International Joint Conference on Neural Networks (IJCNN 2021), Shenzhen, China. <https://doi.org/10.1109/IJCNN52387.2021.9534176>
- Azizah, A., Hashimah, B., Nirmal, K., Siti Zubaidah, A., Puteri, N., Nabihah, A., Sukumaran, R., Balqis, B., Nadia, S. M. R., Sharifah, S. S. S., Rahayu, O., Nur Alham, O., & Azlina, A. A. (2019). *Malaysia national cancer registry report (Report 2012-2016)*. National Cancer Registry. [chrome-extension://efaidnbmnnnibpajpglefindmkaj/https://www.moh.gov.my/moh/resources/Penerbitan/LaporanUmum/2012-2016%20\(MNCRR\)/MNCRR_2012-2016_FINAL_\(PUBLISHED_2019\).pdf](chrome-extension://efaidnbmnnnibpajpglefindmkaj/https://www.moh.gov.my/moh/resources/Penerbitan/LaporanUmum/2012-2016%20(MNCRR)/MNCRR_2012-2016_FINAL_(PUBLISHED_2019).pdf)

- Bertrand, G. (2005). On topological watersheds. *Journal of Mathematical Imaging and Vision*, 22(2), 217-230. <https://doi.org/10.1007/s10851-005-4891-5>
- Bray, F., Ferlay, J., Soerjomataram, I., Siegel, R. L., Torre, L. A., & Jemal, A. (2018). Global cancer statistics 2018: GLOBOCAN estimates of incidence and mortality worldwide for 36 cancers in 185 countries. *CA: A Cancer Journal for Clinicians*, 68(6), 394–424. <https://doi.org/10.3322/caac.21492>
- Camp, B. V. B. (2022). *Data from The Lung Image Database Consortium (LIDC) and Image Database Resource Initiative (IDRI): A completed reference database of lung nodules on CT scans (LIDC-IDRI)*. The Cancer Imaging Archive (TCIA) Public Access. <https://pubmed.ncbi.nlm.nih.gov/21452728/>
- Chin, C. K., Mat, D. A. A., & Saleh, A. Y. (2021a). Hybrid of convolutional neural network algorithm and autoregressive integrated moving average model for skin cancer classification among Malaysian. *IAES International Journal of Artificial Intelligence*, 10(3), 707-716. <https://doi.org/10.11591/ijai.v10.i3.pp707-716>
- Chin, C. K., Mat, D. A. A., & Saleh, A. Y. (2021b, April 9-11). *Skin cancer classification using convolutional neural network with autoregressive integrated moving average*. [Paper presentation]. International Conference on Robot Systems and Applications (ICRSA 2021), Chengdu, China. <https://doi.org/10.1145/3467691.3467693>
- Da Nóbrega, R. V. M., Peixoto, S. A., da Silva, S. P. P., & Rebouças Filho, P. P. (2018, June 18-21). *Lung nodule classification via deep transfer learning in CT lung images*. [Paper presentation]. International Symposium on Computer-based Medical Systems (CBMS 2018), Karlstad, Sweden. <https://doi.org/10.1109/CBMS.2018.00050>
- Forte, G. C., Altmayer, S., Silva, R. F., Stefani, M. T., Libermann, L. L., Cavion, C. C., Youssef, A., Forghani, R., King, J., Mohamed, T. L., Andrade, R. G. F., & Hochegger, B. (2022). Deep learning algorithms for diagnosis of lung cancer: A systematic review and meta-analysis. *Cancers*, 14(16), 3856. <https://doi.org/10.3390/cancers14163856>
- Goodfellow, I., Bengio, Y., & Courville, A. (2016). *Deep learning*. MIT Press.
- Haiying, Y., Zhongwei, F., Ding, D., & Zengyang, S. (2021, May 25-27). *False-positive reduction of pulmonary nodule detection based on deformable convolutional neural networks*. [Paper presentation]. International Conference on Bioinformatics and Computational Biology (ICBCB 2021), Taiyuan, China. <https://doi.org/10.1109/ICBCB52223.2021.9459209>
- Halder, A., Dey, D., & Sadhu, A. K. (2020). Lung nodule detection from feature engineering to deep learning in thoracic CT images: A comprehensive review. *Journal of Digital Imaging*, 33(3), 655-677. <https://doi.org/10.1007/s10278-020-00320-6>
- Keshari, R., Vatsa, M., Singh, R., & Noore, A. (2018, June 18-23). *Learning structure and strength of CNN filters for small sample size training*. [Paper presentation]. IEEE Conference on Computer Vision and Pattern Recognition (CVPR 2018), Utah, USA.
- Li, Z., Yao, H., & Ma, F. (2020, February 3-7). *Learning with small data*. [Paper presentation]. International Conference on Web Search and Data Mining (WSDM 2020), New York, USA.
- Nakrani, M. G., Sable, G. S., & Shinde, U. B. (2021). A comprehensive review on deep learning based lung nodule detection in computed tomography images. In S. C. Satapathy, V. Bhateja, B. & Janakiramaiah, Y. W. Chen (Eds.) *Intelligent system design* (pp.107-116). Springer Link. https://doi.org/10.1007/978-981-15-5400-1_12

- Peirelinck, T., Kazmi, H., Mbuwir, B. V., Hermans, C., Spiessens, F., Suykens, J., & Deconinck, G. (2022). Transfer learning in demand response: A review of algorithms for data-efficient modelling and control. *Energy and AI*, 7, 100126. <https://doi.org/10.1016/j.egyai.2021.100126>
- Primakov, S. P., Ibrahim, A., van Timmeren, J. E., Wu, G., Keek, S. A., Beuque, M., Granzier, R. W. Y., Lavrova, E., Scrivener, M., Sanduleanu, S., Kayan, E., Halilaj, I., Lenaers, A., Wu, J., Monshouwer, R., Geets, X., Gietema, H. A., Hendriks, L. E. L., Morin, O., ... & Lambin, P. (2022). Automated detection and segmentation of non-small cell lung cancer computed tomography images. *Nature Communications*, 13(1), 3423. <https://doi.org/10.1038/s41467-022-30841-3>
- Qin, Y., Zheng, H., Zhu, Y. M., & Yang, J. (2018, April 15-20). *Simultaneous accurate detection of pulmonary nodules and false positive reduction using 3D CNNs*. [Paper presentation]. International Conference on Acoustics, Speech and Signal Processing (ICASSP 2018), Alberta, Canada. <https://doi.org/10.1109/ICASSP.2018.8462546>
- Rajadurai, P., How, S. H., Liam, C. K., Sachithanandan, A., Soon, S. Y., & Tho, L. M. (2020). Lung cancer in Malaysia. *Journal of Thoracic Oncology*, 15(3), 317–323. <https://doi.org/10.1016/j.jtho.2019.10.021>
- Salahuddin, Z., Woodruff, H. C., Chatterjee, A., & Lambin, P. (2022). Transparency of deep neural networks for medical image analysis: A review of interpretability methods. *Computers in Biology and Medicine*, 140, 105111. <https://doi.org/10.1016/j.combiomed.2021.105111>
- Saleh, A. Y., Chin, C. K., Penshie, V., & Al-Absi, H. R. H. (2021). Lung cancer medical images classification using hybrid CNN-SVM. *International Journal Advanced in Intelligence Information*, 7(2), 151-162. <https://doi.org/10.26555/ijain.v7i2.317>
- Sharif, M. I., Li, J. P., Naz, J., & Rashid, I. (2020). A comprehensive review on multi-organs tumor detection based on machine learning. *Pattern Recognition Letters*, 131, 30-37. <https://doi.org/10.1016/j.patrec.2019.12.006>
- Sheng, J., Li, Y., Cao, G., & Hou, K. (2021, July 18-22). *Modeling nodule growth via spatial transformation for follow-up prediction and diagnosis*. [Paper presentation]. International Joint Conference on Neural Networks (IJCNN 2021), Shenzhen, China. <https://doi.org/10.1109/IJCNN52387.2021.9534163>
- Singh, G. A .P., & Gupta, P. K. (2019). Performance analysis of various machine learning-based approaches for detection and classification of lung cancer in humans. *Neural Computing and Applications*, 31(10), 6863–6877. <https://doi.org/10.1007/s00521-018-3518-x>
- Tang, H., Kim, D. R., & Xie, X. (2018, April 4-7). *Automated pulmonary nodule detection using 3D deep convolutional neural networks*. [Paper presentation]. International Symposium on Biomedical Imaging (ISBI 2018), Washington, USA. <https://doi.org/10.1109/ISBI.2018.8363630>
- Tang, S., Yang, M., & Bai, J. (2020). Detection of pulmonary nodules based on a multiscale feature 3D U-Net convolutional neural network of transfer learning. *PLoS One*, 15(8), e0235672. <https://doi.org/10.1371/journal.pone.0235672>
- Thai, A. A., Solomon, B. J., Sequist, L. V., Gainor, J. F., & Heist, R. S. (2021). Lung cancer. *The Lancet*, 398(10299), 535–554. [https://doi.org/10.1016/S0140-6736\(21\)00312-3](https://doi.org/10.1016/S0140-6736(21)00312-3)
- Yamashita, R., Nishio, M., Do, R. K. G., & Togashi, K. (2018). Convolutional neural networks: An overview and application in radiology. *Insights Into Imaging*, 9(4), 611–629. <https://doi.org/10.1007/s13244-018-0639-9>

- Zakaria, R., Abdelmajid, H., & Zitouni, D. (2022). Deep learning in medical imaging: A review. In J. K. Mandal, S. Misra, J. S. Banerjee & S. Nayak (Eds.) *Application of machine intelligence in engineering* (pp.131-144). CRC Press. <https://doi.org/10.1201/9781003269793-15>
- Zhao, X., Liu, L., Qi, S., Teng, Y., Li, J., & Qian, W. (2018). Agile convolutional neural network for pulmonary nodule classification using CT images. *International Journal of Computer Assisted Radiology and Surgery*, 13(4), 585-595. <https://doi.org/10.1007/s11548-017-1696-0>
- Zhuang, F., Qi, Z., Duan, K., Xi, D., Zhu, Y., Zhu, H., ... & He, Q. (2020). A comprehensive survey on transfer learning. *Proceedings of the IEEE*, 109(1), 43-76. <https://doi.org/10.1109/JPROC.2020.3004555>

